Morphological Studies of Glass-Microbead-Filled Polyamide 6.6–Polypropylene Blends

M. ULRICH,[1] C. CAZE,[1] P. LAROCHE[2]

[1] Laboratoire de génie et matériaux textiles (GEMTEX), Ecole Nationale Supérieure des Arts et Industries Textiles, 2 place des martyrs de la résistance, 59070 Roubaix Cedex 1, France

[2] GLAVERBEL Centre de recherche et developpement, 2 rue de l'aurore, 6040 Jumet, Belgium

Received 25 November 1996; accepted 8 July 1997

ABSTRACT: This article deals with the study of the morphology of glass bead (10% in volume) reinforced compatibilized blends of polypropylene (PP) and polyamide (PA) 6.6. The morphology, as well as some physical and mechanical properties, are determined. The blends are studied in relation with the PP–PA ratio and according to the glass bead's sizing. We have seen the existence of a boundary PA–glass beads interface (independently of the sizing), and the best compatibilization effect is obtained with PP size glass beads and for 50% PP content. © 1998 John Wiley & Sons, Inc. J Appl Polym Sci **67:** 201–208, 1998

Key words: polypropylene–polyamide blends; glass bead; sizing; morphology; dynamic mechanical analysis; scanning electron microscopy

INTRODUCTION

Polyamide 6.6–polypropylene (PA 6.6–PP) are very interesting incompatible blends in which PP limits the sensitivity to hydrolysis, while PA contributes to mechanical and thermal properties of the system.

Improvement in properties depends, to a large extent, in the degree of dispersion of the two phases (which depends on the processing conditions, the viscosity of the two phases, the interfacial tension, etc.) and of their composition.

The interfacial tension can be lowered by adding a compatibilizing agent,[1–5] leading to a decrease in the dimension of the dispersed phases, thereby improving some properties, in particular, the resistance to impact if the dispersed phase is an elastomer.[1,6–7]

Filled incompatible polymers blends sometimes presents a heterogeneous distribution of the filler between the components of the blend, for example, black carbon in poly(methyl methacrylate) (PMMA)–polypropylene (PP) and polyethylene (PE)–PP and PE–PMMA[8–9]; calcium carbonate in PE–poly(ethylene, vinyl acetate);[10] calcium carbonate in PP–ethylene–propylene elastomer (EPR);[11] and talc in PP–acrylonitrile–butadiene–styrene copolymer (ABS).[12]

These observations were attributed to a difference in affinity of the filler to each component of the polymer blend; this difference could be linked to the effect of interfacial free energy[8,11] or to chemical interactions between the filler and one of the components of the blend[10]; and encapsulation of the filler by one of the components of the blend can occur.

For glass fiber-reinforced polymers blends, we can have a specific interaction of the glass fibers with one of the component of the blend[13] or a random distribution of the glass fibers in the two phases of the blend.[14]

Correspondence to: C. Caze.

Journal of Applied Polymer Science, Vol. 67, 201–208 (1998)
 CCC 0021-8995/98/020201-08

In previous work,[15] we have observed that surface treatment of the glass fibers can influence the morphology of the reinforced polymer blend. This property can be used to enhance the performance of reinforced polymers blends, for example, the PA 6.6–PP–glass fiber blends present in relation to the glass fiber treatment, particular morphologies, and very interesting properties.[15–16]

This article deals with the study of glass-bead-reinforced PA 6.6–PP blends. Glass beads are introduced in the mixture in order to observe their effects on the morphology of the blend according to their surface treatment or sizing and to study the interphase compatibilization (the interphase compatibilization was observed for glass-bead-reinforced PA 6–PP blends[17]). We will show that the glass bead's sizing affects the morphology of the blend in the areas near the beads and influences the mechanical properties.

EXPERIMENTAL PROCEDURE

Materials

The polypropylene (PP) used was manufactured by Hoechst (Hostalen PPN 1060). It was blended in variable proportions with Zytel E101 LNC101, a 6.6 polyamide (PA 6.6) from Du Pont. The coupling agent was a PP functionalized by maleic anhydride (Polybond 3002 from BP Chemicals), added in a proportion of 2.5% by weight of the amount of PP. The blends will be referred by their polyamide percentages in volume, as follows: 0PA, 20PA, 40PA, 50PA, 60PA, 80PA, and 100PA.

The two glass beads that we were studied were produced and sized by Glaverbel (Belgium), and they differed in the nature of their sizing. One, 40A1, is PP-sized (alkyl silane as coupling agent); while the other, 40GF20, is normally used to reinforce polyamide (amino silane as coupling agent). This two types of glass beads have about the same high surface energy; for 40A1 and 40GF20, the γ values are 60 ($\gamma^d_{\mathrm{GBPP}} = 20$; $\gamma^p_{\mathrm{GBPP}} = 40$) and 50 dynes cm^{-1} ($\gamma^d_{\mathrm{GBPA}} = 20$; $\gamma^p_{\mathrm{GBPA}} = 30$), respectively; these glass beads will be referred to as GBPP and GBPA, respectively. They had an initial diameter of 40 μm in average.

Processing

The polymer matrix was obtained by introducing granules of each constituent at the head of a Baker Perkins MP 2030 double-screw extruder. The glass beads were subsequently added to the fused polymer mixture and represented 10% in volume of the final complex (about 20–25% by weight). No accurate dosage was checked by pyrolysis. The resulting granules (Grinder Baughan 1316) were dried for 12 h in a circulating dried air oven, Motan MD 11, at 85°C. The samples used in the mechanical tests were injection molded with a Boy 15 S.

Mechanical Properties

Eight samples of each blend were systematically tested to obtain the mean value. The tests were performed on dried specimens. The stress–strain curves were recorded at ambient temperature on a Zwick machine type 1446, with a strain rate of 5 mm/min.

Electronic Microscopy

The tensile fractures surfaces were observed after gold palladium plating, using a Jeol Jem CX120 scanning electron microscope. We also examine the surfaces of microtomes cut in the bulk, before and after dissolving the PP phase in boiling xylene at 140°C for 2 h.

Differential Scanning Calorimetry (DSC)

The characteristics of the crystallization of PP and PA 6.6 in the blends were studied on DSC7 (Perkin–Elmer). The temperature of the sample was increased to 300°C, in closed aluminum pans, for 5 min to fuse the polymers. Peak crystallization was recorded during cooling at a rate of 40°C min under nitrogen gas. The temperature of the pure PP samples were only increased to 200°C for 5 min. Crystallinity was calculated from the heat observed of crystallization, with the assumption that ΔH for PP and PA are 209 and 196 J/g, respectively, in a complete crystalline state.

Dynamic Mechanical Analysis (DMTA)

The T_g values of PA 6.6 was determined using a Polymer Laboratories DMTA MK III. Each specimen was subjected to a flexural stress using a clamped bending mode (dual cantilever). The typical geometry of the samples are as follows: $l = 30$, $w = 12$, $t = 3$ mm, free length = 14 mm, $\log k = 2w(t/l)^3$. The temperature of the samples was increased from −55 to 200°C (PP pure) and from −55 to 265°C for the PP–PA blends, at a rate of 5°C/min (this choice of heating rate, associated to

thick samples, leads to a shift of the T_g values towards higher temperatures). Moreover, in order to prevent water absorption during the experiment, we also determined the glass transition (T_g) of the polyamide using special dried samples (80°C per 72 h in an air-dried oven). In this case, the temperature of the samples was increased from 20 to 265°C at a rate of 2°C min.

The elastic modulus E', the viscous modules E'', and their ratio E''/E' (loss tangent δ) curves were recorded at 0.3 Hz. The glass transition temperature is taken at the maximum of the G'' curve.

Determination of the PA Phase Location Around the Glass Beads

Half part of one injection molded sample is filled, then dyed red with a common textile PA acid dyeing. PA is a polymer that dyes well contrary to PP. The dyeing used is a Nilosane N red 2RBL made by Sandoz at a concentration of 0.2% by weight. The dyed surfaces were observed using an optical microscope connected to a computer and its scan analyzer software through a TV camera. All PA/PP blends were analyzed, as well as samples of PP, PP reinforced by glass beads without coupling agent, and blends of PP and Polybond. The observations are concentrated around the beads: a red coloration indicates the presence of an amount of PA.

RESULTS AND DISCUSSION

Morphologies of the Blends

PA Location Using Red Dyeing

We have observed all the colored samples using an optical microscope in order to distinguish the red color at several magnifications (100, 200, and 400×). Pure PP, as well as blends of PP and Polybond and PP filled with glass beads, are not dyed. The PA, with their acid chemical end groups, is a polymer that dyes well contrary to the PP one.

As seen in Figure 1 and for the blends with PA, the polymer around the beads has always been red-dyed. Observations are only possible for slight percentages of PA (20PA, 40PA). Over these percentages, the concentration of dyeing is too high on the surface, and no difference is visible. We observed that over 95% of the beads, whatever the sizing, are surrounded with red dyeing. We conclude that the two kinds of glass beads are preferentially recovered with PA, and this is as soon as PA is incorporated in the blend.

This location can be explained by the surfaces tensions values; in melt, we have $\gamma = 20.8$ ($\gamma^p = 0$) for PP and $\gamma = 28.3$ ($\gamma^p = 9.6$, $\gamma^d = 18.7$) for PA. Applying eq. (1),[18] we can evaluate the interfacial tension (dynes cm), as follows:

$$\gamma_{1/2} = \gamma_1 + \gamma_2 - 2(\gamma_1^p \cdot \gamma_2^p)^{1/2} - 2(\gamma_1^d \cdot \gamma_2^d)^{1/2} \quad (1)$$

where $\gamma_{PP/PA} = 11$, $\gamma_{PP/GBPP} = 90.1$, $\gamma_{PA/GBPP} = 40.3$, $\gamma_{PP/GBPA} = 80.1$, and $\gamma_{PA/GBPA} = 30.3$.

From the interfacial values, we can now calculate the spreading coefficient (1 and 2 refer to the polymers, and GB refers to glass beads) from equation (2).[19] This coefficient gives the behavior of the polymers in competition for the filler, as follows:

$$\lambda_{1/GB} = \gamma_{2/GB} - \gamma_{1/GB} - \gamma_{1/2} \quad (2)$$

If $\lambda_{1/GB}$ and $\lambda_{2/GB} > 0$, then there is a competition between 1 and 2; and both spread on GB. If $\lambda_{1/GB} > 0$ and $\lambda_{2/GB} < 0$, then only 1 spreads on GB. From the following values, determined before: $\lambda_{PA/GBPP} = 8$ and $\lambda_{PP/GBPP} = -30$, then PA spreads on the GBPP glass beads, $\lambda_{PA/GBPA} = 18.5$ and $\lambda_{PP/GBPA} = -40.5$, then PA spreads on the GBPA glass beads, we can conclude that PA surrounded the glass beads. In this calculation, we have neglected the effect of the compatibilizing agent; in fact, this agent decreases the interfacial energy between the two polymers $\gamma_{1/2}$; at the maximum, it can annul $\gamma_{1/2}$, but the conclusion does not change.

Microscopy

The photomicrographs (Fig. 2) were produced after dissolving the PP phase in boiling xylene for 2 h.

At low PA content, we can make the same observation for all the blends independently of the glass bead's sizing; we find nodules of PA around the beads, which are growing according to the percentage of PA (20PA and 40PA). We can observe a continuous PA phase at lower PA content with PA glass bead's sizing (50%) than with PP glass bead's sizing (60%).

For 60 and 80 PA blends, we don't see nodules of PP polymer in the PA matrix; so we can conclude that both PA and PP polymers form a bicontinuous phase.[2,18,20]

Conclusions

From the PA location and the MEB observation, we have the following.

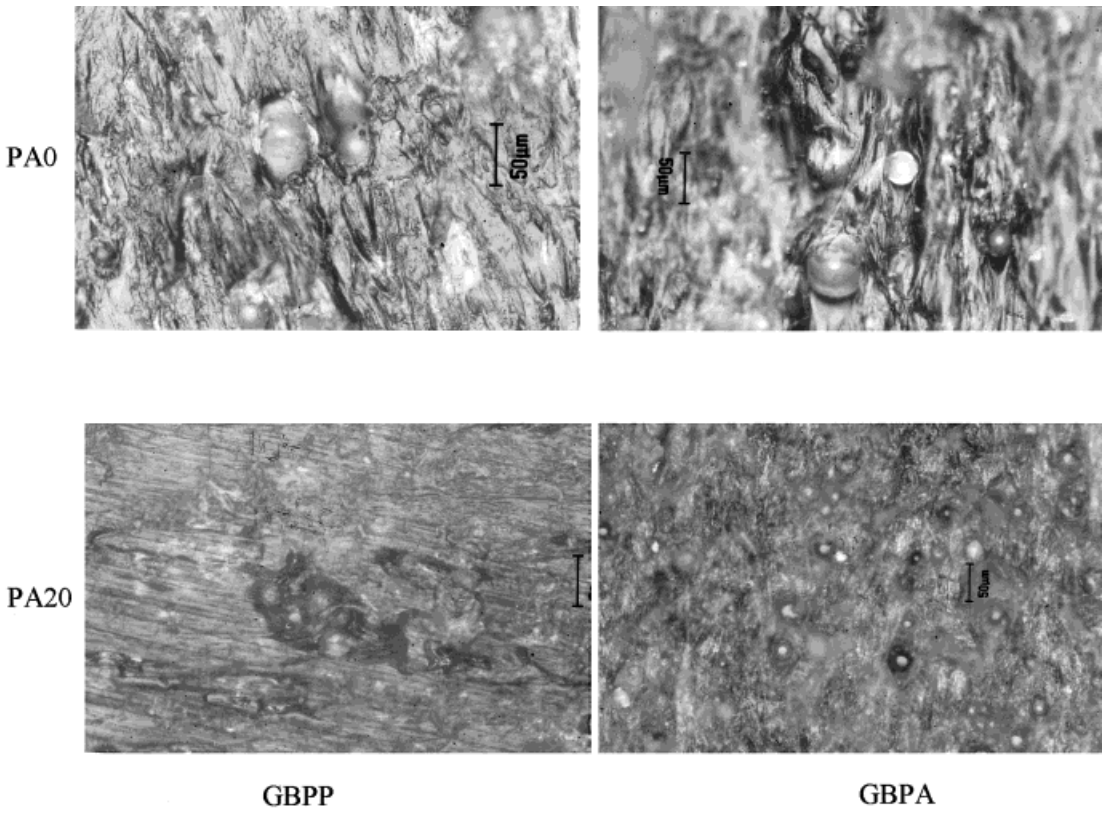

Figure 1 PA location by dyeing.

1. Independently of the glass bead's sizing and of the PA content, all the blends show beads surrounded with PA.
2. At low PA content, we have nodules of PA in the PP matrix.
3. When the PA content increases, we have fusion of the nodules with formation of a continuous PA phase. This continuous PA phase is formed at lower PA content with PA glass bead's sizing (50%) than with PP glass bead's sizing (60%).

Glass Transition and Degree of Crystallinity of PA in the Blends

Glass Transition

As can be seen in Table I, the evolution of the T_g of the PA phase is quite similar, whatever the sizing, except for the 20PA blend. For this last one, the T_g value increases tremendously: 76.6°C for GBPP; and 78.4°C for GBPA compared to 73.5°C ± 0.5°C for all the other blends. We noted also that the PA T_g for GBPA and GBPP are in the same order for a PA content in the blends greater than 50%.

As seen previously, independently of the glass bead's sizing and of the PA content, all the blends present beads surrounded with PA, so we have formation of a boundary interphase (BI)[21] between the PA and the microbeads. The effect of this BI depends on the relative percentage of PA in the BI so the effect should be more important at low PA content. It leads to a decrease of the mobility of the PA chain and so to an increase of the PA T_g values, which is experimentally observed for GPPA and GBPP.

Contrary to GBPP, GBPA can present chemical reaction with PA,[22] leading to a more restrictive mobility of the PA chain in the BI and, as a consequence, explaining the higher PA T_g value obtained for the GBPA blends for a PA content in the blends lower than 50%.

Degree of Crystallinity

As we can see in Table I, the degree of crystallinity (DC) of PA is independent of the PA content and

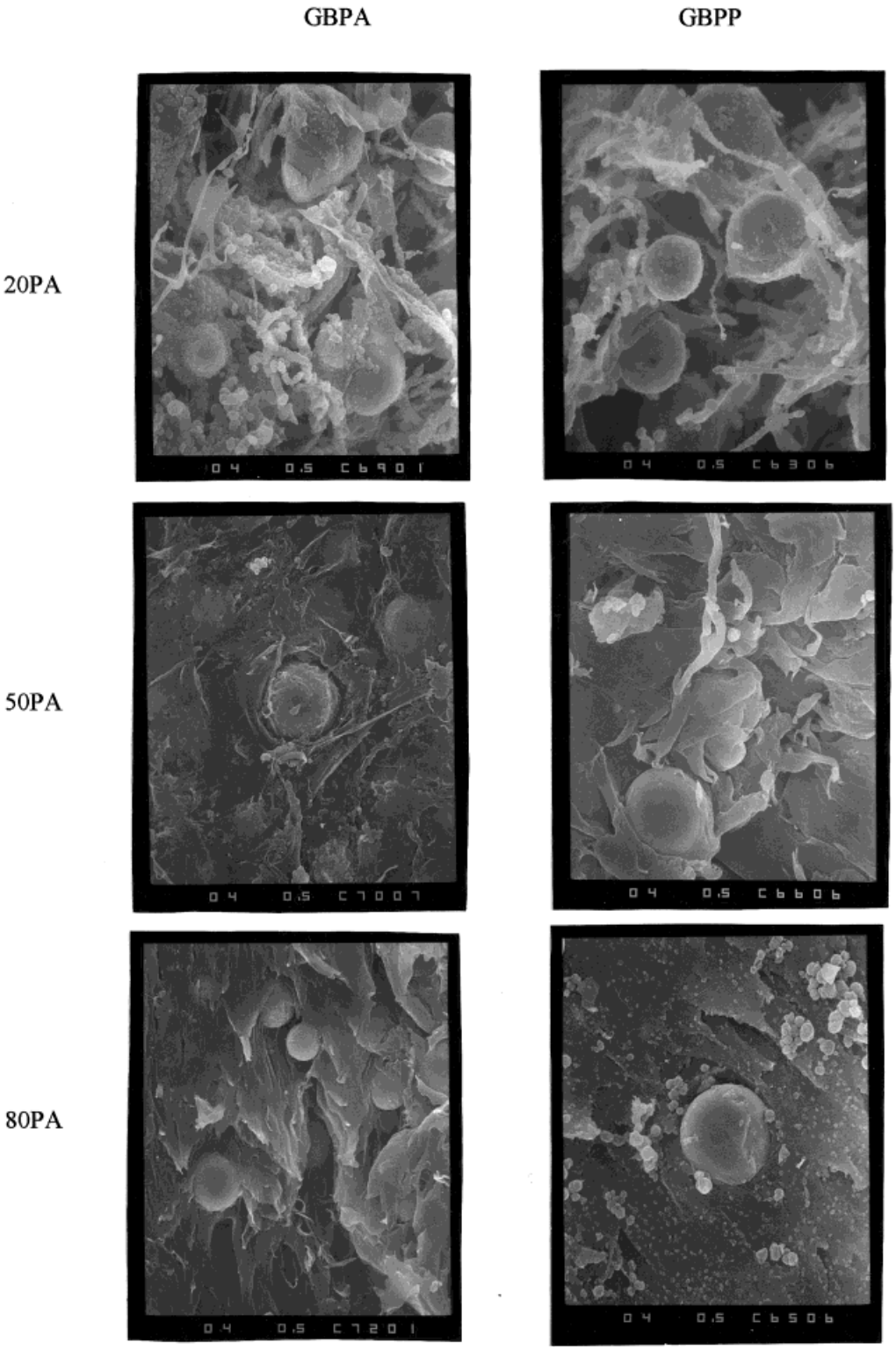

Figure 2 Scanning electron microscopy of GBPA and GBPP blends (×500).

Table I Evolution of the Characteristics of the Blends

	PA T_g		PA Crystallinity		PP Crystallinity	
PA %	GBPP	GBPA	GBPP	GBPA	GBPP	GBPA
0					43.5	45.3
20	76.6	78.4	21.5	19.2	45.3	42.3
40	73.9	74.2	29.4	28.9	42.3	41.7
50	73.6	73.9	28.6	28.0	40.0	41.3
60	73.5	73.4	27.9	27.5	43.3	40.9
80	73.3	73.6	29.2	28.2	41.7	39.2
100	73.1	73.5	30.3	30.6		

the glass bead's sizing, except for the blends with low PA content (20%). This observation, as for the evolution of the PA T_g value, can be linked to the existence of a BI, which leads to a decrease of the DC.[8]

Degree of Crystallinity of PP in the Blends

As can be seen in Table I, the DC of the PP (0% PA) depends on the glass bead's sizing: 43.5% for GBPP and 45.3% for GBPA. This observation can be related to a compatibilization at the interphase PP–glass beads by the alkyl chain of the coupling agent with GBPP rather than with GBPA, leading to a decrease of the degree of crystallinity of the polymer.[23]

The evolution of the DC of PP in the blends filled with GBPA show a decrease in the DC of PP; this observation can be related to the action of the compatibilizing agent; the alkyl chain of the Polybond 3002 induces a restricted chain arrangement of the PP matrix.

The situation is more complex for the blends filled with GBPP. For the blend at 20% PA, the DC of PP increases and is greater than the corresponding blend filled with GBPP. This can be due to the following.

1. The introduction of PA. The PA modified the interface GB–PP (as seen previously, all the blends present beads surrounded with PA) and induced a decrease of the compatibilization at the interphase.
2. The location of the Polybond 3002. The compatibilizing agent is linked to the PA chain; so in the GB area, we have a competition for the Polybond 3002 between the PP chain and the alkyl chain of the silane coupling agent.

The best compatibilization effect (for all the blends) is observed when a continuous PA phase is obtained (around 50%). For the Blends at 60 and 80% PA, the increase of DC is probably due to the competition of the Polybond for the glass bead and the PP because we have a decrease of the ratio of Polybond-to-(PP + glass beads).

Mechanical Properties

The evolution of the Young's modulus and of the ultimate tensile strength versus the PA content are reported in Figure 3. Their evolution shows clearly the formation of a PA continuous phase at around 50% of PA. The blends filled with GBPA always gives the best mechanical properties, except for the 50–60% PA content area, where the blends filled with GBPP are better. This can be explained by the previous conclusion on the evolution of the degree of crystallinity; these blends presents the best compatibilization effect.

CONCLUSION

A number of polyamide 6.6–polypropylene blends were reinforced with two types of glass bead: one with a sizing suitable for polypropylene; the other for polyamide. In all the blends that were investigated, the glass beads were always coated with polyamide (independently of the sizing used), leading to the creation around the glass bead of a boundary interphase. The properties of the blends can be explained by its morphologies and the existence of this boundary interface.

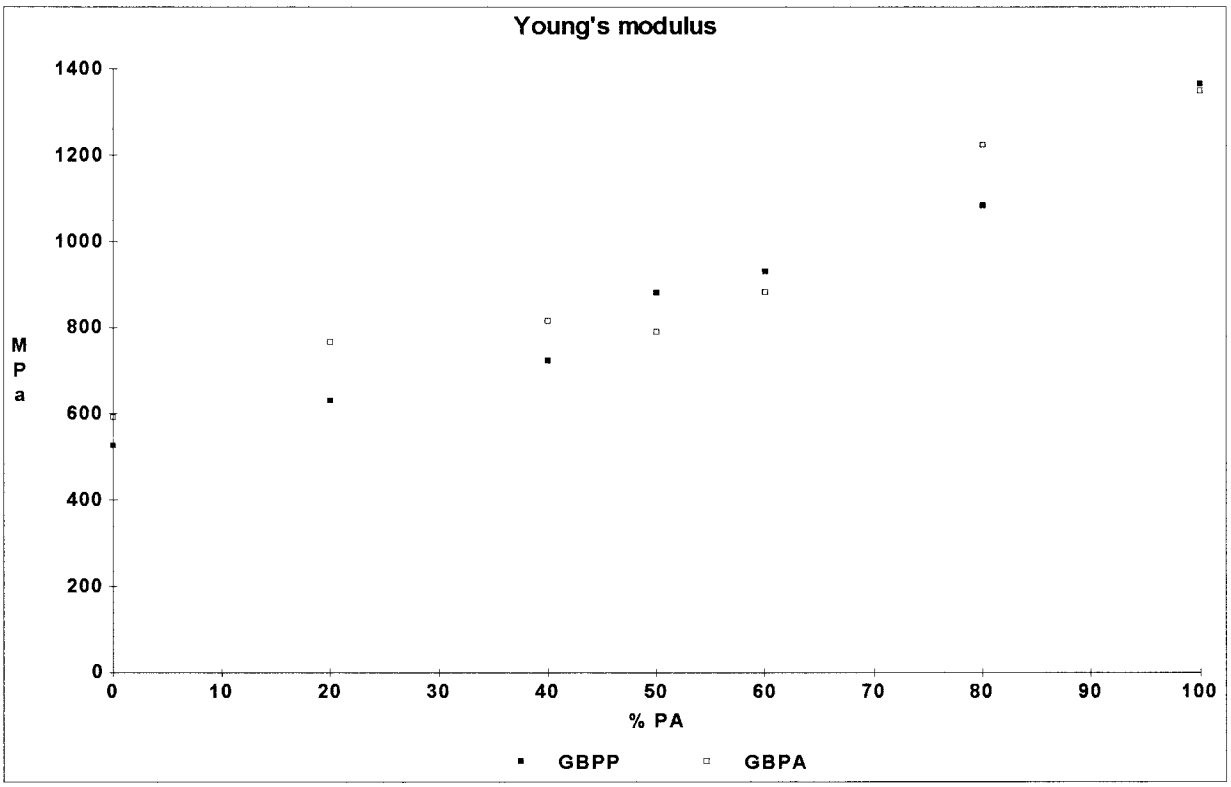

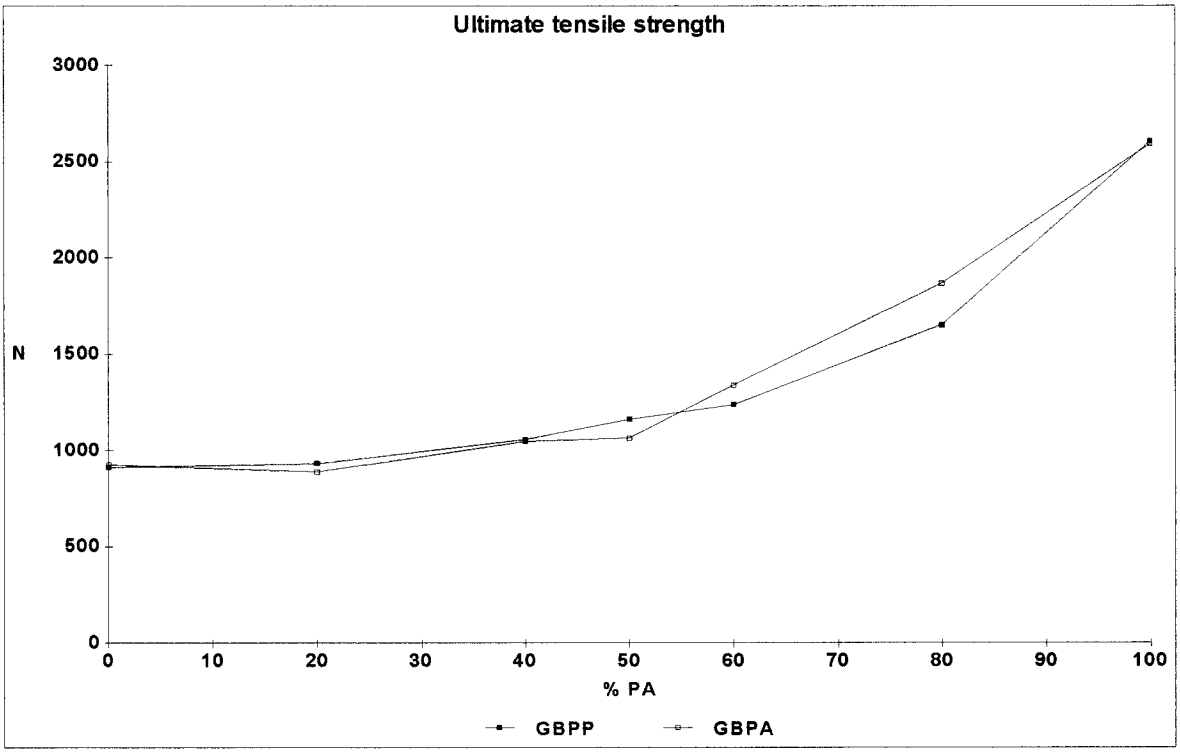

Figure 3 Young's modulus and ultimate tensile strength of the PA–PP blends as a function of their compositions and for the two kinds of sizing.

The authors thank L. Brunet from Centre Commun de Microscopie Electronique (University of Lille 1) for SEM pictures.

REFERENCES

1. R. Greco, M. Malincinico, E. Martuscelli, G. Ragosta, and G. Scarinzi, *Polymer,* **28,** 1185 (1987).
2. San Jin Park, Byung Kyu Kim, and Han Mo Jeong, *Eur. Polym. J.,* **26,** 131 (1990).
3. F. Ide and A. Hasegawa, *J. Appl. Polym. Sci.,* **18,** 963 (1974).
4. J. M. Willis, V. Caldas, and D. B. Favis, *J. Mater. Sci.,* **26,** 4742 (1991).
5. P. V. Gheluwe, B. D. Favis, and J. P. Chalifoux, *J. Mater. Sci.,* **23,** 3910 (1988).
6. S. Wu, *Polymer,* **26,** 1855 (1985).
7. A. Crespy, C. Caze, D. Coupe, P. Dupont, and J. P. Cavrot, *Polym. Eng. Sci.,* **32,** 273 (1992).
8. S. Asai, K. Sakata, M. Sumita, and K. Miyasaka, *Polym. J.,* **24,** 415 (1992).
9. M. Sumita, K. Sakata, Y. Hayakawa, S. Asai, K. Miyasaka, and M. Tanemura, *Colloid. Polym. Sci.,* **270,** 134 (1992).
10. K. Mitsuishi, S. Kodoma, and H. Kawasaki, *Polym. Comp.,* **9,** 112 (1988).
11. J. Kolarik and J. Jancar, *Polymer,* **33,** 4961 (1992).
12. W. Jingwu and Z. Chengshen, *Suliao,* **19,** 3 (1990).
13. M. Avella, P. Greco, E. Martuscelli, G. Orsello, and E. Bertotti, *J. Mater. Sci.,* **27,** 4131 (1992).
14. D. R. Saini and J. M. Schultz, *Polym. Comp.,* **10,** 222 (1989).
15. A. Perwuelz, C. Caze, and W. Piret, *J. Thermoplas. Comp. Mater.,* **6,** 176 (1993).
16. D. Benderly, A. Siegmann, and M. Narkis, *J. Mater. Sci. Lett.,* **14,** 132 (1995).
17. H. Ischida and N. Scherbakoff, *Makromol. Chem., Macromol. Symp.,* **50,** 157 (1991).
18. D. K. Owens and R. C. Wendt, *J. Appl. Polym. Sci.,* **13,** 1741 (1969).
19. A. W. Adamson, *Physical Chemistry of Surfaces,* 5th ed., Marcel Dekker, New York, 1990.
20. B. Maxwell and L. J. Guillermo, *Polym. Eng. Sci.,* **23,** 614 (1983).
21. V. P. Privalko and V. V. Novikov, *The Science of Heterogeneous Polymers,* Wiley, 1995.
22. T. P. Huijgen, H. Angadgaur, T. L. Weeding, L. W. Jenneskens, H. E. C. Schuurs, W. G. B. Huysmans, and W. S. Veeman, *Macromolecules,* **23,** 3063 (1990).
23. W. J. Mackight and R. W. Lenz, *Polym. Eng. Sci.,* **25,** 1124 (1985).